Metrol. Meas. Syst., Vol. 29 (2022) No. 4, pp. 685–700
DOI: 10.24425/mms.2022.143067

PAN POLSKA AKADEMIA NAUK

METROLOGY AND MEASUREMENT SYSTEMS
Index 330930, ISSN 0860-8229
www.metrology.wat.edu.pl

M&MS

DESIGN AND EVALUATION OF A LOW-COST SOLAR SIMULATOR AND MEASUREMENT SYSTEM FOR LOW-POWER PHOTOVOLTAIC PANELS

Marcin Walczak[1)], Leszek Bychto[1)], Jarosław Kraśniewski[1)], Stanisław Duer[2)]

1) *Koszalin University of Technology, Department of Electronics and Computer Science, Faculty of Electronics, 2 Śniadeckich St., 75-453 Koszalin, Poland* (✉ *marcin.walczak@tu.koszalin.pl*, +48 94 3478 708, *leszek.bychto@tu.koszalin.pl*, *jaroslaw.krasniewski@tu.koszalin.pl*)
2) *Koszalin University of Technology, Department of Energy, Faculty of Mechanical Engineering, 15–17 Racławicka St., 75-620 Koszalin, Poland* (*stanislaw.duer@tu.koszalin.pl*)

Abstract

Research related to photovoltaic panels comprises different topics starting with modelling solar cells, finding new maximum power point tracking (MPPT) algorithms, testing existing ones or designing of DC/DC converters for MPPT systems and microgrids that incorporate photovoltaic energy sources. In each of the examples above a deep knowledge of photovoltaic panels is required, as well as a reliable measurement system that can deliver continuous, stable light with enough power to meet standard test conditions (STC) and that can ensure repeatable results. Therefore this paper presents a low-cost solar simulator with a microcontroller-based measurement system, that can be used for various measurements of low-power photovoltaic panels.

Keywords: solar simulator, photovoltaic panels, photovoltaics, measurements of PV panel characteristics, MPPT evaluation.

1. Introduction

The problem of energy production, especially the so-called green energy, has been emphasised over the last few years. A fair amount of papers focuses on *photovoltaic* (PV) panels as one of the green energy sources that do not cause any pollution, do not generate any noise, and that can be utilized for energy harvesting on a small scale – such as powering small devices using solar cells operating at the waste light [1]. A lot of research on PV panels concerns their electrical characteristics as well as maximum power point tracking algorithms [2–8]. However, many research papers that propose new algorithms include simulations only, which is helpful with getting quick results, but if a new idea is put forward, at some point it should be verified by physical model and measurements. To measure electric characteristics of a PV panel or to test a maximum power point tracking algorithm a stable light source is required to illuminate

Article history: received June 9, 2022; revised August 10, 2022; accepted August 11, 2022; available online September 26, 2022.

the panel's surface with relatively unified light. The sunlight provides high uniformity, but the irradiance is changing constantly causing some difficulties with getting repeatable results of the measurements. Moreover, it is difficult to keep control over the temperature of a PV panel under the sunlight, which can impact I–V characteristics even more [9, 10]. A solution to overcome the problems would be using a commercial solar simulator. However, such devices are expensive and a large part of their spectrum does not contribute to the total output power of a PV panel due to its spectrum sensitivity [1]. Therefore, many researchers have searched for an alternative and designed their own solar simulators using different types of light sources to evaluate PV panels and *maximum power point tracking* (MPPT) algorithms under stable and controlled conditions. Among the simulators there can be found devices which incorporate LED lights [11] to measure dynamic properties of PV panels. Halogen lamps are usually used to measure I–V characteristics, but because they emit a lot of heat. They are also used to evaluate cooling methods in PV panels [12–16] and hybrid systems [17, 18]. Additionally, there exist mixed solar simulators which utilize both LEDs and halogen lamps [19, 20], but the cost of such simulators is correspondingly higher. Basically, halogen lamps are commonly used because of their low cost and light spectrum which does not contain significant spikes and is similar to the spectral response of a solar cell [1, 21, 22].

The goal of this paper is to propose and evaluate a measurement system that incorporates a solar simulator, consisting of halogen lamps and a microcontroller-based device to measure voltages and currents of a PV panel. The whole system has already been used in previous work [23] and it ought to be useful in future research.

Section 2 of this paper includes a general concept, detailed description of the system, and used materials. Section 3 contains results of measurements including the range of the solar simulator irradiance, light spectrum, heating curve of the PV panel, dynamics of the light source, the performance of the measurement system and comparison between power characteristics measured with the solar simulator and directly under the sunlight.

2. Materials and methods

This section includes information on design and technical features of the irradiator and the measurement system. Since the system consists of many modules working together, they will be described separately in the following subsections. The main idea of the measurement system is presented in Fig. 1. It consists of an irradiator, a DC/DC converter, a microcontroller with dedicated sensors, and a computer.

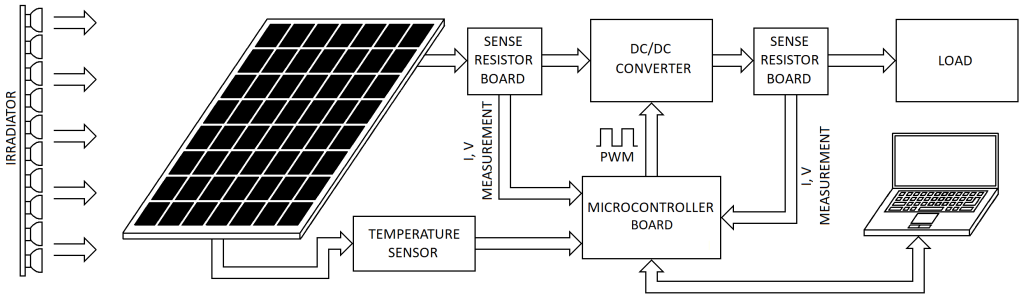

Fig. 1. Simplified block diagram of the irradiator and measurement system for low-power photovoltaic panels.

Metrol. Meas. Syst., Vol. 29 (2022), No. 4, pp. 685–700
DOI: 10.24425/mms.2022.143067

The irradiator provides a substantial amount of the light power to a PV panel. The DC/DC converter can change its input resistance based on the *Pulse-width Modulation* (PWM) signal fed to the converter's transistor. Therefore, it is used to move the operating point of the panel across its I–V characteristics. The microcontroller generates the PWM signal, measures the input/output voltages and currents of the DC/DC converter, measures the temperature of the PV panel and sends all of the relevant data to the computer, where they are processed and presented on the screen.

2.1. Solar simulator (irradiator)

Measurements of a PV panel's I–V characteristics as well as evaluation of different MPPT algorithms require a relatively stable and powerful light source that can imitate the sun light according to *standard test conditions* (STC) (*i.e.* 1000 W/m^2). The stability of the light source is required to avoid current oscillations which, if present during the measurement, would affect the I–V characteristics and would make MPPT algorithms hard to evaluate or compare to each other. The power of the irradiator should be regulated to enable measurements for different irradiance levels.

Some designs of solar simulators can be found in the literature [11–20]. In [1] authors measured the spectra of a few light sources and came up with a conclusion that incandescent and halogen bulbs emit light that is comparable to the sunlight spectrum. Moreover, these bulbs produce light in which the most of the energy is in the range of the monocrystal and polycrystal PV panels sensitivity and therefore they are the best choice as regards illuminating PV panels.

At first, 230 VAC halogen bulbs were taken into consideration, but in that case the light might flicker due to the alternating current (Fig. 2a) and thus influence MPPT algorithm evaluation. This problem can be solved by using switching power supplies – the reason is that the incandescent lights have relatively low dynamics, therefore a few kilohertz switching signal should not affect the light amplitude (Fig. 2b). Such a solution would require building a high power AC/DC converter (or group of converters) that would be able to feed the bulbs with enough power to achieve the standard test conditions. Apart from elimination of the flickering problem, the converter would enable regulation of the irradiance. A drawback of using 230 V halogen bulbs is the safety issue, therefore the irradiator presented in this paper was built using 12 V halogen bulbs.

a) b)

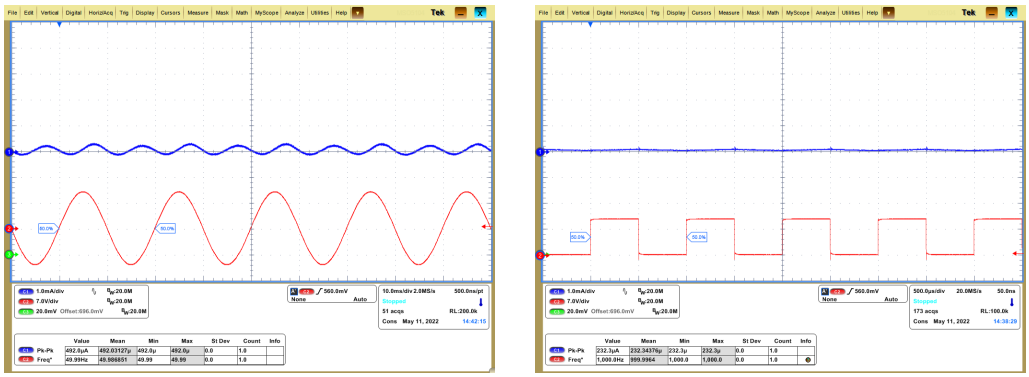

Fig. 2. Current of a PV panel illuminated with a halogen bulb powered with a) 10 Vpp, 50 Hz sinusoidal voltage; b) 10 V, 1 kHz square voltage.

To build the irradiator 180 of 50 W halogen light bulbs (15 × 12) were used. They were arranged in a way that reminds of the structure of a honeycomb to minimize free spaces between the bulbs as shown in Fig. 3a. The distance between the centres of any two adjacent bulbs is approximately 52 mm as shown in Fig. 3b.

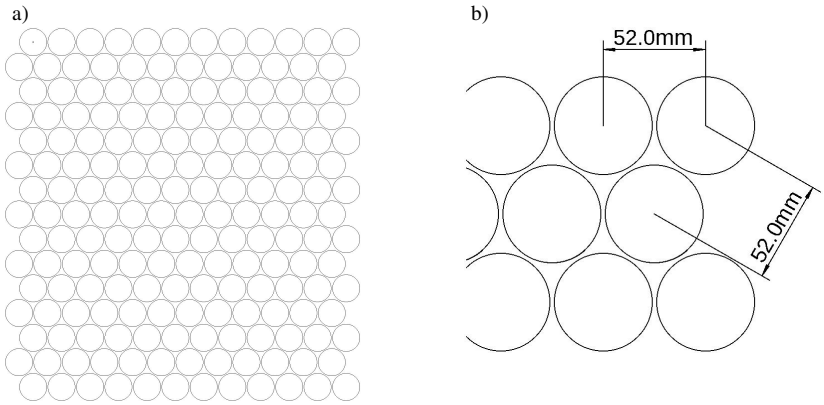

Fig. 3. Arrangement of halogen bulbs in the irradiator.

The beam angle of a single bulb is 60°, which is relevant in terms of the light distribution when multiple bulbs are placed next to each other – this topic will be described in details later in this paper. The irradiator is powered from an Agilent 6692A DC power supply that enables smooth regulation of the output power. The power supply can continuously provide between 0-60 V and 0-110 A, which in theory translates to 6600 W of maximum power. In reality, because of the bulb resistance, the output voltage and current reach only 34 V and 110A with all bulbs turned on. This translates to 3470 W of power and over 1000 W/m^2 of the irradiance, which is enough to provide standard test conditions for a PV panel.

2.2. Microcontroller board

The microcontroller board is used for PWM signal generation, measurements and communication with a computer application. The microcontroller can measure the temperature of a PV panel as well as the input/output voltage and current. It utilizes a PIC32MZ1024 microcontroller with a built-in 12-bit analogue to digital converter, an UART transceiver and a 16-bit PWM generator. The PWM generator can produce signals with a wide range of frequencies. One bit of the generator corresponds to 17.86 ns, therefore the smallest frequency, that can be generated, is around 855 Hz. The highest possible frequency depends on the required resolution of the duty cycle. In the case of a 100 kHz signal, the duty cycle resolution is around 0.2%, whereas with a 1 MHz signal the resolution drops to around 1.8%.

To communicate with the computer the microcontroller uses an ADUM1201CRZ digital isolator, placed on the board, and an FT232RL transceiver. Thanks to the isolator, the transceiver and the USB port are protected from too high voltage that could appear in case of a system failure. Moreover, the electrical isolation enables applying the microcontroller board to multiple PV panels, connected in series, without the need to take care of different voltage levels as shown in Fig. 4.

Metrol. Meas. Syst., Vol. 29 (2022), No. 4, pp. 685–700
DOI: 10.24425/mms.2022.143067

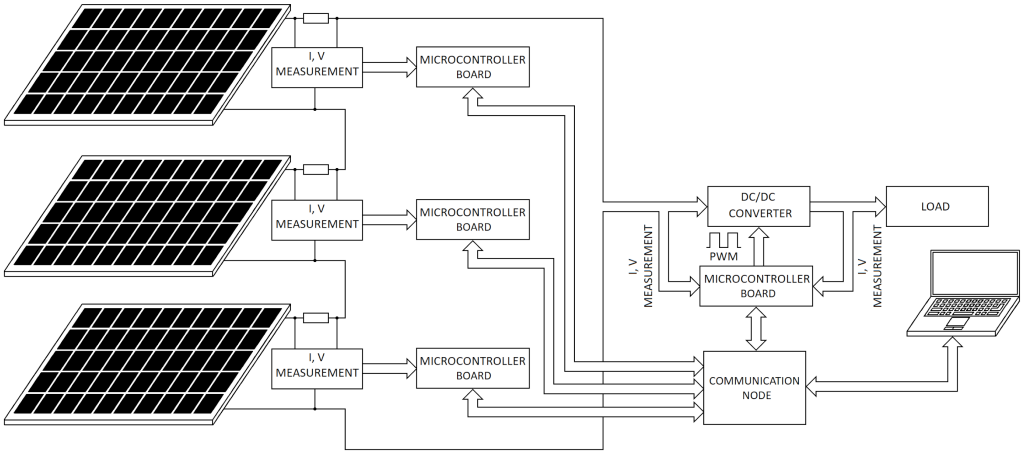

Fig. 4. Example of microcontroller board application in a series connection of PV panels.

The temperature of a panel is determined with a MAX6675 external 12-bit thermocouple sensor that can measure the temperature with a resolution of 0.25°C. After every change of the duty cycle the temperature, voltages and currents are sent to the computer via the USB port.

The input/output voltages and currents are measured using the peripheral 12-bit analogue to digital converter. The signals are fed to the ADCs via voltage dividers and INA180 differential amplifiers respectively. The current is measured as a voltage drop across a 20 mΩ sense resistor (Fig. 5). The value of the resistor is relatively small to reduce the influence of the resistor on the system efficiency. The resolution of the voltage and current measurements is 6.299 mV and 0.4395 mA respectively. The maximum values that can be measured are 25.8 V and 1.8 A by default. However, the whole system was divided into modules, which are placed on separate PCBs, to enable testing and quick component replacement. Therefore, the actual maximum voltages and currents are not fixed and can change based on the application.

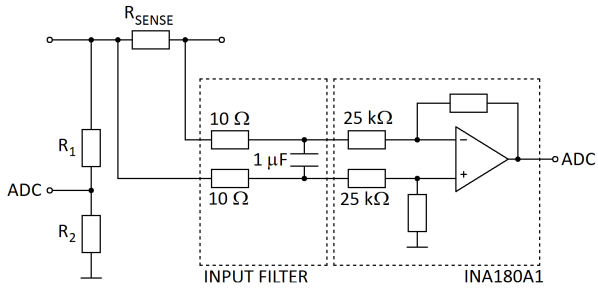

Fig. 5. Voltage and current measurement.

Usually, the measured currents and voltages contain high-frequency harmonics due to the PWM signal that continuously switches a converter's transistor on and off. The harmonics affect the measured signals often creating a non-sinusoidal distortions (Fig. 6) that are difficult to measure using a microcontroller with a limited sampling rate and calculation power.

a)

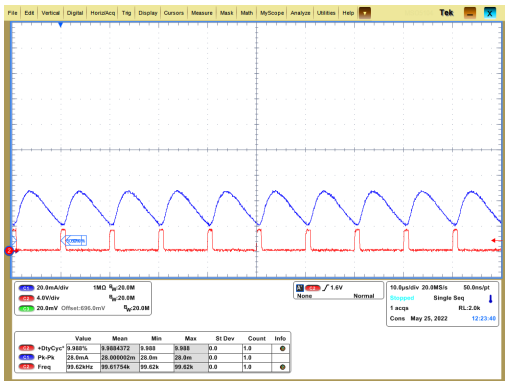

b)

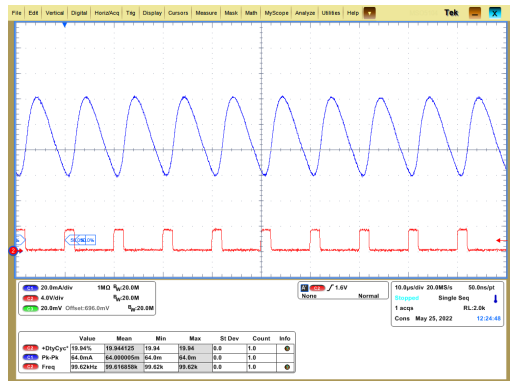

c)

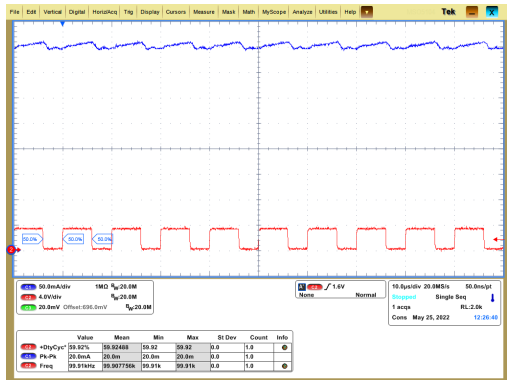

Fig. 6. Input current of a DC/DC converter connected to a PV panel:
a) $D = 0.1$; b) $D = 0.2$; c) $D = 0.6$.

Additionally, the measured signal may contain high frequency noise (far beyond the switching frequency) which complicates the measurement even more. The system has to be prepared for such situations, therefore an input filter was applied at the input of the differential amplifier to reduce the impact of the high-frequency harmonics on the input/output current measurements. The filter components were chosen following the datasheet guidelines according to which the 10 Ω value of the filtering resistor (Fig. 5) introduces a gain error of 0.99%, which is an acceptable value. Additionally, to get rid of fluctuations in the measured value, and at the same time increase the repeatability of each measurement, the microcontroller calculates the average values of the signals. The calculations are based on the instantaneous values of the voltages and currents that are measured 14 times per switching cycle (in the case of 100 kHz PWM), throughout 100 cycles (which takes about 1 ms). The result is then divided by the total number of samples, which gives an averaged value over one switching period.

The resistors used for the voltage divider have the tolerance of 0.1%, therefore in the worst case scenario the total error related to the voltage measurement can reach up to 0.186% ±LSB, which is also an acceptable value.

Metrol. Meas. Syst., Vol. 29 (2022), No. 4, pp. 685–700
DOI: 10.24425/mms.2022.143067

2.3. DC/DC converter

For testing purposes a DC/DC buck converter was designed. The converter is presented in Fig. 7, whereas its parameters are presented in Table 1. The inductor value was chosen to provide relatively low current ripple and low *equivalent series resistance* (ESR). Higher values of the inductance would increase transient response time, which would translate to extended time of maximum power point tracking, and thus lower the efficiency of the MPPT system [24]. The model of the converter, describing the input current response to a duty cycle perturbation is presented in equations (1)–(8) [25]. The model describes the input current of the converter working in the *continuous conduction mode* (CCM) and includes all parasitic resistances, which was proven to be relevant in terms of transient time calculations [25].

$$I_\theta(s) = \left.\frac{I_g(s)}{\theta(s)}\right|_{V_g(s)=0}, \tag{1}$$

$$I_\theta(s) = \frac{D_A V_Z\,(sC_Z + G)}{s^2 LC_Z + s\,(LG + R_Z C_Z + CR_C) + GR_Z + 1} + I_L\,, \tag{2}$$

$$V_O = \frac{D_A V_G + V_D\,(1 - D_A)}{GR_Z + 1}\,, \tag{3}$$

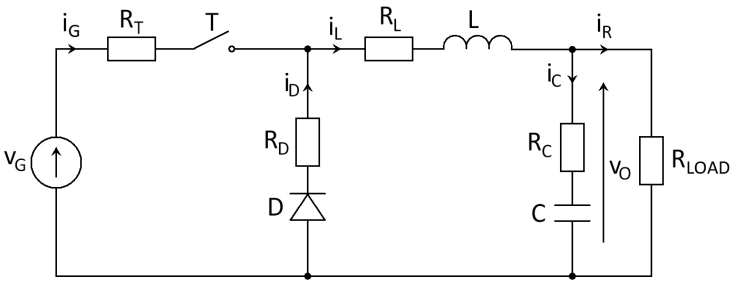

Fig. 7. DC/DC buck converter used for the measurement system.

Table 1. Parameters of the converter used during the measurements.

Name	Symbol	Value	Unit
Inductance	L	47	µH
Output capacitance	C_O	100	µF
Input capacitance	C_{IN}	10	µF
Load resistance	R_{LOAD}	10	Ω
Inductor equivalent series resistance (ESR)	R_L	76	mΩ
Capacitor equivalent series resistance (ESR)	R_C	200	mΩ
Diode	D	MBRS340T3	–
Diode static resistance	R_{D}	285	mΩ
Transistor	T	IPB60R099C6	–
Transistor on resistance	$R_{\mathrm{DS(ON)}}$	99	mΩ

$$I_L = V_O G\,, \tag{4}$$

$$V_Z = V_G + (R_D - R_T)\, I_L\,, \tag{5}$$

$$R_Z = D_A\,(R_T - R_D) + R_L + R_D\,, \tag{6}$$

$$C_Z = C\,(1 + G R_C)\,, \tag{7}$$

$$G = \frac{1}{R_{\mathrm{LOAD}}}\,, \tag{8}$$

where: I_g – small signal value of the converter's input current, V_O – quiescent value of the output voltage, I_L – quiescent value of the inductor current.

The input current of a DC/DC buck converter is interrupted due to the converter's topology. Therefore, an input capacitor has to be introduced to the converter. The capacitor filters high-frequency harmonics and provides relatively constant current on the output of the PV panel. However, the value of this capacitor should be lower than the value of the output capacitor, otherwise an instability can occur [26].

3. Results

3.1. Irradiator

3.1.1. Irradiance

The irradiator was built using halogen lamps as shown in Fig. 3. The dimensions of the irradiator are 625 × 680 mm which translates to the total area of 0.425 m^2. The halogen lamps are powered by the DC power supply. The irradiance level can be changed using different input voltages as shown in Fig. 8. The figure shows that the standard test conditions of 1000 W/m^2 can be achieved at the distance of 165 mm from the irradiator.

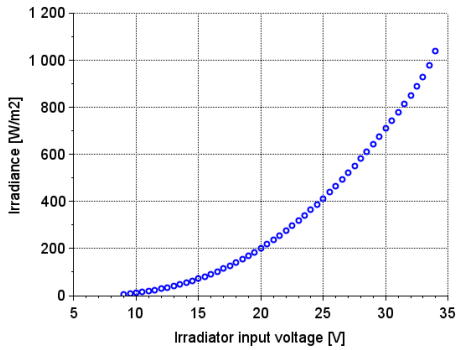

Fig. 8. Irradiance of the irradiator in function of the irradiator input voltage.

A change in the irradiance level influences the wavelength spectrum (as shown in Fig. 9). However, when the irradiance curve is calibrated the changes become irrelevant in terms of the power generated by the PV panel. Nevertheless, the spectrum of the halogen bulbs can be relevant in the case of PV panels other than those made of silicon.

Metrol. Meas. Syst., Vol. 29 (2022), No. 4, pp. 685–700
DOI: 10.24425/mms.2022.143067

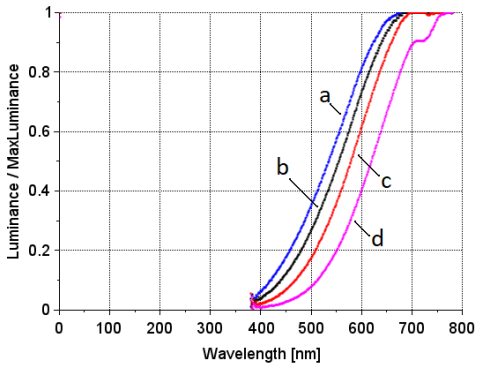

Fig. 9. Unified spectrum of the irradiator light for different input voltages (measured with a Konica Minolta CS-2000): a – 45 V, b – 35 V, c – 25 V, d – 15 V.

3.1.2. Heating effect

The irradiator generates high amounts of heat (especially for higher irradiance levels) therefore another aspect that has to be addressed is the heating of the PV panel during a measurement. Fig. 10 shows how the panel heats up while illuminated using halogen lamps with the irradiance of 1000 W/m^2. One can see that the change in the temperature is relatively slow *i.e.* a 1°C change takes around 2 seconds, whereas a single measurement of the voltages and currents takes less than 1 ms (in the case of the converter used in the experiment). The measurement itself is short enough to reduce the risk of heating up the panel. Additionally, the measurement is done during short periods of time in which the PV panel is illuminated. After the measurement is done the light is turned off and the panel can cool down while the parameters, such as irradiance level or load resistance, are changed.

Regarding the dynamics of the light source – when powered up the irradiator takes some time to reach the steady-state point which can take about 1 second as shown in Fig. 11. During that time the system should not take any measurements due to the changing irradiance. This additional delay can slightly influence the temperature of the PV panel. However, in that case the change would be relatively small and thus acceptable.

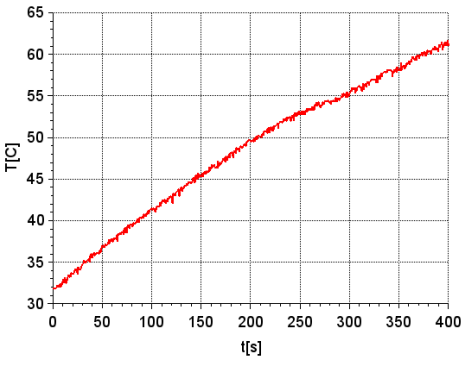

Fig. 10. PV panel temperature change in time (for irradiance level 1000 W/m^2).

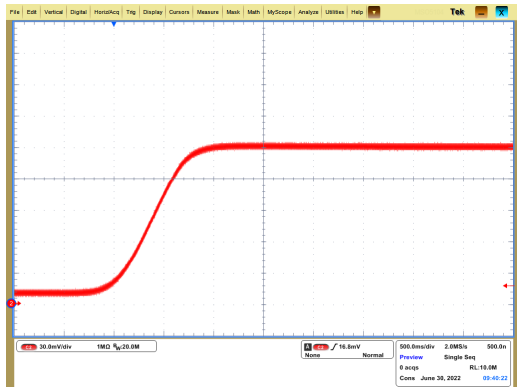

Fig. 11. Voltage across light detector Thorlabs PDA36A after a change of the irradiator's input voltage.

3.2. Voltage and current measurements

The input/output current and voltage measurements are performed using the microcontroller's analog-to-digital converters connected to a differential amplifier and a voltage divider respectively. The differential amplifier measures the voltage drop on a relatively small sense resistor, as shown in Fig. 5. The input filter of the amplifier reduces the high-frequency harmonics that are present in the input current, which translates to reduced transient oscillations and a lower amplitude of the AC component in the steady state condition.

Experimental data presenting the amplifier's output voltage response to a perturbation of the duty cycle, for different input filters, are presented in Fig. 12a–12c, whereas the effect of the input filter on the amplifier's output voltage in the steady state condition is presented in Fig. 13a–13c.

a) b)

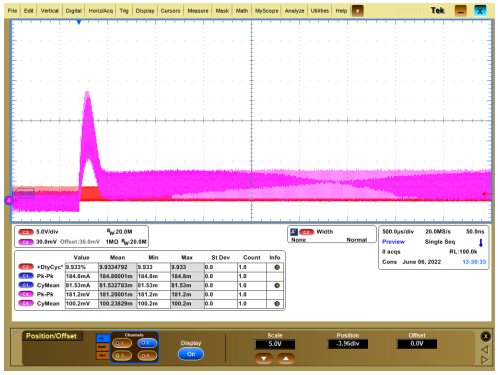

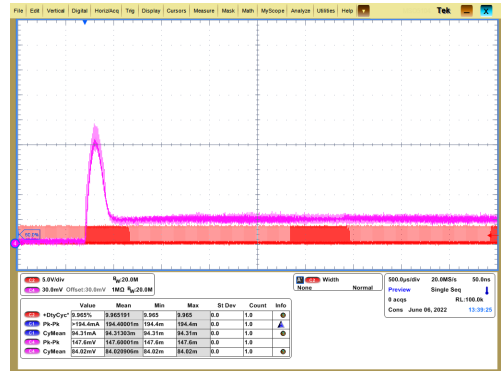

c)

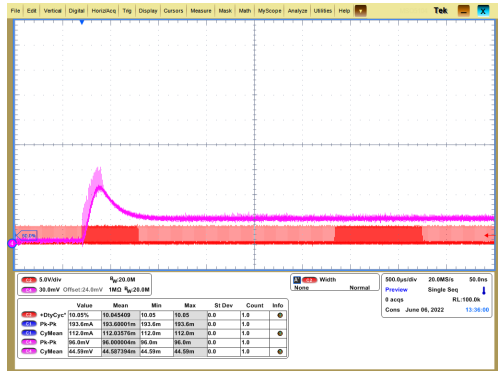

Fig. 12. Differential amplifier's output voltage response to a perturbation of the duty cycle; a) without an input filter; b) with a 10 Ω, 1 µF input filter, (c) with a 10 Ω, 10 µF input filter.

The oscillogram in Fig. 12a shows the input current of the DC/DC converter that was measured with a TCP0030A current probe. The current features a high overshoot after a step change of the duty cycle which proves that the current should be measured with some delay. The amplifier's input filter reduces the switching frequency harmonic, providing a signal that is easier to measure

Metrol. Meas. Syst., Vol. 29 (2022), No. 4, pp. 685–700
DOI: 10.24425/mms.2022.143067

a) b)

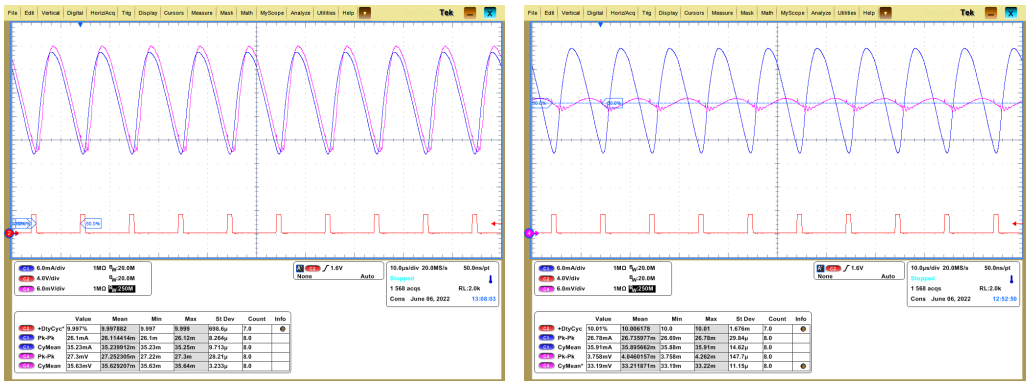

c)

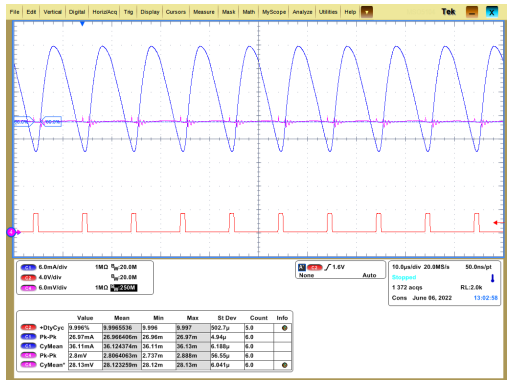

Fig. 13. Differential amplifier's output voltage in steady state; a) without an input filter; b) with a 10 Ω, 1 µF input filter; c) with a 10 Ω, 10 µF input filter.

(Fig. 12b). The 10 Ω and 10 µF filter (Fig. 12c) reduces the overshoot even more but at the same time it influences the total time of transients, therefore it is up to debate if it should be used in fast MPPT systems. More details regarding the filtration of the switching frequency harmonic can be seen on Fig. 13 where the input current was measured using a differential amplifier with different input filters, but this time in steady state conditions to show the current oscillations.

It can be noticed that the amplifier's input filter reduces the amplitude of the switching frequency oscillations, and thus enables more precise measurements of the input current. However, even though the amplitude of the oscillations is reduced, some high frequency spikes can be noticed on the oscillograms. The spikes are in correlation with the rising and falling edge of the PWM signal and can be the source of differences between the measured and the real value of the input current. Therefore, apart from the input filter an additional feature in the form of averaging of measured samples has been introduced to the system, as mentioned in Section 2.2. The averaging reduces the influence of random noise on the measured values and enables measurements with the accuracy of the least significant bit (LSB).

Additionally, the system enables the user to choose the number of the averaged samples and the time delay between the duty cycle change and the first sample, which enables more control over the measurement (especially when converters with different parameters are used).

3.3. Measurement system

The measuring set is presented in Fig. 14. The microcontroller board can be powered with voltage in the range of 4–12 V. The PV panel is connected to the input of the first sense resistor board (Fig. 14c), the output of the board is connected to the DC/DC converter, which subsequently is connected to the load via second sense resistor board. The temperature sensor (Fig. 14d) is optional, however, it enables measurements of PV panel temperature. The irradiator is presented in Fig. 15.

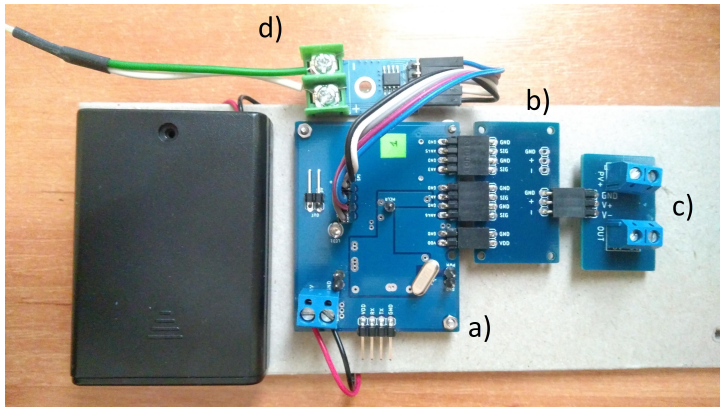

Fig. 14. Measurement system incorporating: a) the microcontroller board; b) voltage divider/differential amplifier board; c) sense resistor board; d) temperature sensor.

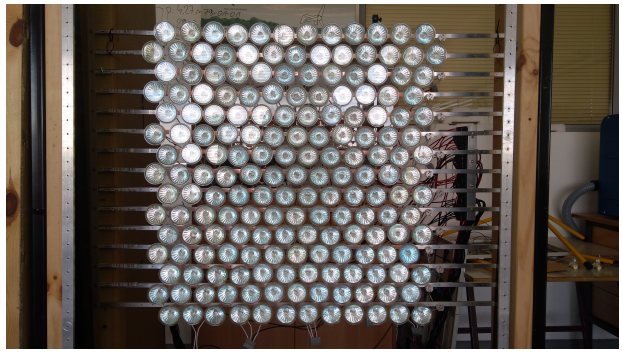

Fig. 15. Irradiator built with 180 × 50 W halogen lamps.

The distance of around 165 mm between the irradiator and the PV panel has been chosen experimentally – first the I–V characteristics of the panel had been measured under the sunlight. Next, similar measurements were performed using the irradiator for different distances (the input voltage of the halogen lamps had been modified for each distance, to keep the irradiance level

Metrol. Meas. Syst., Vol. 29 (2022), No. 4, pp. 685–700
DOI: 10.24425/mms.2022.143067

relatively constant). Finally, the characteristics were compared and the best match between the measurements under the sun and the irradiator determined the best distance between the irradiator and the PV panel. The final results of the measurement are presented in Fig. 16a where the solid lines represent the measurements under the sunlight, whereas the dashed lines represent the measurements with the irradiator at a distance of 165 mm from the bulbs. In contrast, when not all halogen bulbs were turned on, the power characteristics of the panel, under the irradiator light, were deformed as shown in Fig. 16b. This shows how important the uniformity of the light is.

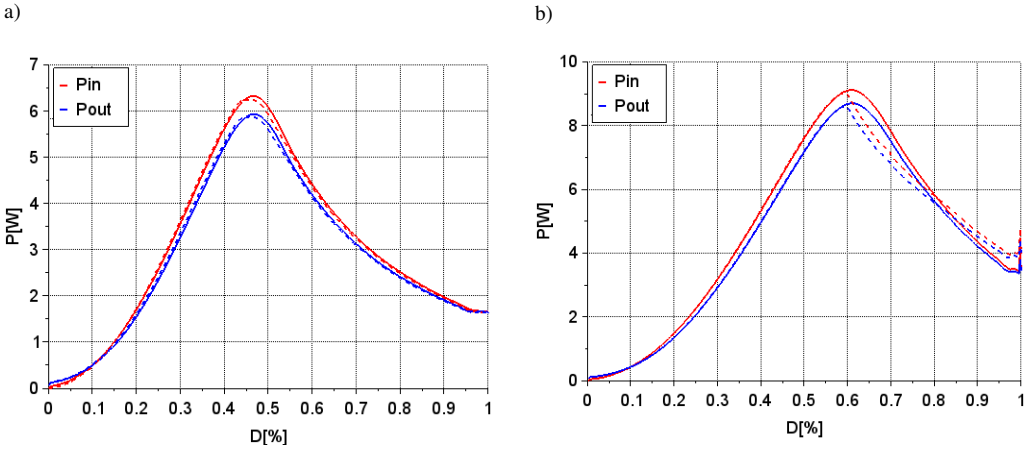

Fig. 16. Measurement of the input and output power of the buck converter connected to a 10 W PV panel and a resistive load of 10 ohms: solid lines represent measurements under the sunlight, dashed lines represent measurements under the irradiator light.

4. Discussion

In general, the measurement system consists of two devices – the irradiator and the microcontroller board with the computer program.

The irradiator consists of halogen bulbs that had been proven to have the best spectrum to imitate the sunlight, among other light sources [1]. The irradiator can emit light with the maximum irradiance of 1000 W/m^2, which complies with the standard test conditions, and thus can be used to evaluate photovoltaic panels for the maximum power available during the day. Because the irradiator has limited dimensions, in its current form it can be used to evaluate only low power photovoltaic panels – panels with larger surface area can be expected to have uneven light distribution at the distance of 165 mm which can lead to deformed characteristics as shown in Fig. 16b. Better uniformity can be achieved for larger distances but at the cost of the maximum irradiance power. As shown in Fig. 16a, the system enables measurements that are in consistency with the measurements done directly under the sunlight. It confirms that the irradiator can be used for PV panel measurements and after increasing the total numbers of bulbs it can be used to illuminate PV panels of higher power. The bulbs used for the system have the power of 50 W each, which probably is the reason why the power supply cannot reach its full output power. To solve this problem halogen bulbs with smaller power (*i.e.* higher resistance) should be used.

The microcontroller board with the computer program is used to set the measurement parameters and measure the input/output currents and voltages of a DC/DC converter. With 12-bit

resolution of the ADC and the averaging feature it enables measurements with acceptable accuracy of 1 LSB. The maximum measurable voltage and current can be changed by connecting a different voltage divider/differential amplifier board. Its modular design enables using external devices, such as the 16-bit INA226, to measure currents and voltages with higher resolutions. The temperature sensor enables a better control over the measurement process. The system provides one PWM signal output, that can be used for all asynchronous converters. It can also be used with synchronous converters by incorporating a special driver with the dead time feature, such as IR2184, but to get a full control over the PWM signals an additional PWM output is required, therefore it is recommended to provide one when designing such system.

In the presented example a single measurement took about 1 ms, which enables relatively fast measurement of panel characteristics. The measurement time is limited by the transients and the number of samples used for averaging. Nevertheless, 1 ms per single point measurement is enough to avoid large temperature changes caused by the irradiance, even when large number of measurement points is required. It is important to point out that the duration of the transiens changes with the duty cycle, therefore an additional feature can be added to the system to reduce the total time of the measurement.

5. Conclusions

The solar simulator enables measurements of different electrical parameters of a PV panel, such as the I–V characteristics, power characteristics, influence of the temperature on the power curves, testing maximum power point tracking algorithms and efficiency of the DC/DC converter used. Designing a measurement system to measure I–V characteristics of a photovoltaic panel requires overcoming some problems related to the presence of a noise, transients and stability of a light source. The system presented in this paper enables reliable measurements with the ADC resolution of 12bit and the accuracy of the least significant bit. It provides a stable light source which is crucial in order to get repeatable results, and thus evaluate panel characteristics or test an MPPT algorithm. It can be stated that the measured characteristics of PV power vs the duty cycle for the sunlight and the irradiator are consistent as shown in Fig. 16a. The differences between the characteristics are minor and irrelevant in terms of future research.

References

[1] Górecki, K., Dąbrowski, J., & Krac, E. (2021). Modeling Solar Cells Operating at Waste Light. *Energies*, *14*(10), 2871. https://doi.org/10.3390/en14102871

[2] Karami, N., Moubayed, N., & Outbib, R. (2017). General review and classification of different MPPT Techniques. *Renewable and Sustainable Energy Reviews*, *68*(1), 1–18. https://doi.org/10.1016/j.rser.2016.09.132

[3] Banu, I.V., Beniugă, R., & Istrate, M. (2017, October 18). Comparative Analysis of the Perturb-and-Observe and Incremental Conductance MPPT Methods. *2013 8th International Symposium on Advanced Topics in Electrical Engineering (ATEE)*. https://doi.org/10.1109/ATEE.2013.6563483

[4] Mostafa, H. H., Ibrahim, A. M., & Anis W. R. (2019). A performance analysis of a hybrid golden section search methodology and a nature-inspired algorithm for MPPT in a solar PV system. *Archives of Electrical Engineering*, *68*(3), 611–627. https://doi.org/10.24425/aee.2019.129345

Metrol. Meas. Syst., Vol. 29 (2022), No. 4, pp. 685–700
DOI: 10.24425/mms.2022.143067

[5] Mroczka, J., & Ostrowski, M. (2014). A Hybrid Maximum Power Point Search Method Using Temperature Measurements in Partial Shading Conditions. *Metrology and Measurement Systems*, *21*(4), 733–740. https://doi.org/10.2478/mms-2014-0056

[6] Akram, N., Khan, L., Agha, S., & Hafeez, K. (2022). Global Maximum Power Point Tracking of Partially Shaded PV System Using Advanced Optimization Techniques. *Energies*, *15*(11), 4055. https://doi.org/10.3390/en15114055

[7] Chavan, V. C., Mikkili, S., & Senjyu, T. (2022). Hardware Implementation of Novel Shade Dispersion PV Reconfiguration Technique to Enhance Maximum Power under Partial Shading Conditions. *Energies*, *15*(10), 3515. https://doi.org/10.3390/en15103515

[8] Khan, M. J., Kumar, D., Narayan, Y., Malik, H., García Márquez, F. P., & Gómez Muñoz, C. Q. (2022). A Novel Artificial Intelligence Maximum Power Point Tracking Technique for Integrated PV-WT-FC Frameworks. *Energies*, *15*(9), 3352. https://doi.org/10.3390/en15093352

[9] Xiao, W., Ozog, N. & Dunford, W.G. (2007). Topology Study of Photovoltaic Interface for Maximum Power Point Tracking. *IEEE Transactions on Industrial Electronics*, *54*(3), 1696–1704. https://doi.org/10.1109/TIE.2007.894732

[10] Padhee, S., Pati, U. C., & Mahapatra, K. (2016, August). Design of photovoltaic MPPT based charger for lead-acid batteries. *2016 IEEE International Conference on Emerging Technologies and Innovative Business Practices for the Transformation of Societies (EmergiTech)*, (pp. 351–356). https://doi.org/10.1109/EmergiTech.2016.7737365

[11] Qin L., Xie, S., Yang C., & Cao J. (2013, June). Dynamic model and dynamic characteristics of solar cell. *2013 IEEE ECCE Asia Downunder,* (pp. 659–663). https://doi.org/10.1109/ECCE-Asia.2013.6579170

[12] Tanesab, J., Ali, M., Parera, G., Mauta, J., Sinaga1, R. (2019, October). A Modified Halogen Solar Simulator. *ICESC 2019*, (pp. 18–19). http://dx.doi.org/10.4108/eai.18-10-2019.2289851

[13] Al Mansur A., Islam, M. I., ul Haq, M. A., Maruf, M. H., Shihavuddin, A., & Amin, M. R. (2020, December). Investigation of PV Modules Electrical Characteristics for Laboratory Experiments using Halogen Solar Simulator. *2020 2nd International Conference on Sustainable Technologies for Industry 4.0 (STI)*. https://doi.org/10.1109/STI50764.2020.9350496

[14] Wajs, J., Golabek, A., & Bochniak, R. (2019). Photovoltaic Roof Tiles: The Influence of Heat Recovery on Overall Performance. *Energies, 12*(21), 4097. https://doi.org/10.3390/en12214097

[15] Wajs, J., Golabek, A., Bochniak, R., & Mikielewicz, D. (2020). Air-cooled photovoltaic roof tile as an example of the BIPVT system – An experimental study on the energy and exergy performance. *Energy, 197*, 117255. https://doi.org/10.1016/j.energy.2020.117255

[16] Sarniak, M. T. (2021). The Efficiency of Obtaining Electricity and Heat from the Photovoltaic Module under Different Irradiance Conditions. *Energies, 14*, 8271. https://doi.org/10.3390/en14248271

[17] Kalogirou, S. A., & Tripanagnostopoulos, Y. (2006). Hybrid PV/T solar systems for domestic hot water and electricity production. *Energy Conversion and Management 47*(24), 3368–3382. https://doi.org/10.1016/j.enconman.2006.01.012

[18] Moharram, K. A., Abd-Elhady, M. S., Kandil, H. A., & El-Sherif, H. (2013). Enhancing the performance of photovoltaic panels by water cooling. *Ain Shams Engineering Journal, 4*(4), 869–877. https://doi.org/10.1016/j.asej.2013.03.005

[19] Grandi, G., Ienina A., & Bardhi, M. (2014). Effective low-cost hybrid LED-halogen solar simulator. *IEEE Transactions on Industry Applications, 50*(5), 3055–3064. https://doi.org/10.1109/TIA.2014.2330003

[20] Namin, A., Jivacate, C., Chenvidhya, D., Kirtikara, K., & Thongpron, J. (2012). Construction of Tungsten Halogen, Pulsed LED, and Combined Tungsten Halogen-LED Solar Simulators for Solar Cell-Characterization and Electrical Parameters Determination. *International Journal of Photoenergy*, 2012. https://doi.org/10.1155/2012/527820

[21] Dafalla, Y., & Osman, M. (2016, October). A solar simulator for the Renewable Energy instruction laboratory. *2016 IEEE Conference on Technologies for Sustainability (SusTech)*, (pp. 235–239). https://doi.org/10.1109/SusTech.2016.7897173

[22] Esen, V., Sağlam, Ş., & Oral, B. (2017). Light sources of solar simulators for photovoltaic devices: A review. *Renewable and Sustainable Energy Reviews, 77*, 1240–1250. https://doi.org/10.1016/j.rser.2017.03.062

[23] Walczak, M., & Bychto, L. (2021). Influence of Parasitic Resistances on the Input Resistance of Buck and Boost Converters in Maximum Power Point Tracking (MPPT) Systems. *Electronics, 10*(12), 1464. https://doi.org/10.3390/electronics10121464

[24] Yilmaza, U., Turksoyb, O., & Tekec, A. (2019). Improved MPPT method to increase accuracy and speed in photovoltaic systems under variable atmospheric conditions. *International Journal of Electrical Power and Energy Systems, 113*, 634–651. https://doi.org/10.1016/j.ijepes.2019.05.074

[25] Janke, W., Bączek, M., Kraśniewski, J., & Walczak, M. (2022). Input Small-Signal Characteristics of Selected DC–DC Switching Converters. *Energies*, *15*, 1924. https://doi.org/10.3390/en15051924

[26] Hayat, A., Faisal, A., Javed, M. Y., Hasseb, M., & Rana, R. A. (2016, April). Effects of Input Capacitor (Cin) of Boost Converter for Photovoltaic System. *2016 International Conference on Computing, Electronic and Electrical Engineering (ICE Cube), Quetta*, (pp. 68–73). https://doi.org/10.1109/ICECUBE.2016.7495257